ORIGINAL ARTICLE
DOI: https://doi.org/10.30932/1992-3252-2023-21-5-4

World of Transport and Transportation, 2023,
Vol. 21, Iss. 5 (108), pp. 192–203

Optimisation of the Design of an Underwater Floating Transport Structure

Ivan M. DEMIDOV **Vladimir Yu. POLIAKOV**

Ivan M. Demidov [1],
Vladimir Yu. Poliakov [2]
[1, 2] *Russian University of Transport Moscow, Russia.*
✉ [2] *pvy55@mail.ru.*
[1] *Russian Science Citation Index SPIN-code: 3365-6643.*
[2] *Scopus Author ID: 57201723559, Web of Science ID: AAS-4866-2021.*

ABSTRACT

The article considers the optimisation of internal forces from constant loads of the underwater floating transport structure to reduce the local effects of internal forces.

This new type of structures can be used at significant depths of intersected water obstacles. Such structures will be in demand for the construction of underwater crossings as part of transcontinental transport corridors such as North – South, Japan – Europe and others.

The purpose of the proposed study is to optimise the design to solve the problem of overloads of structural elements. To solve this problem, methods of structural mechanics and numerical experiment using the finite element method were used. Optimisation makes it possible to reduce bending moments in the zones of the edge effect when using a radial fastening scheme by several times. This will allow the use of unified sections of the structure. The article substantiates optimisation methods and their verification using the finite element method.

The article also discusses the problems of system survivability of a structure in the event of failure of one or two anchorages. Bending moments increase significantly, but the traffic could be continued since the load from the train and the sum of constant loads have opposite signs.

Keywords: transport construction, submerged floating tunnel, SFT, optimisation, radial fastening, deep-sea obstacles.

For citation: Demidov, I. M., Poliakov, V. Yu. Optimisation of the Design of an Underwater Floating Transport Structure. World of Transport and Transportation, World of Transport and Transportation, 2023, Vol. 21, Iss. 5 (108), pp. 192–203. DOI: https://doi.org/10.30932/1992-3252-2023-21-5-4.

The text of the article originally written in Russian is published in the first part of the issue.
Текст статьи на русском языке публикуется в первой части данного выпуска.

INTRODUCTION

Underwater floating transport tunnels represent a new type of transport structures with several significant advantages [1]. The most important of them are the possibility of construction at significant water depths, as well as compensation for the weight of the structure by the pushing Archimedean force for positive buoyancy. Positive buoyancy, which prevents diving to a depth higher than the calculated one, should also be provided during the passage of the rolling stock. Therefore, a temporary load from the train will probably reduce the internal forces in the elements of the structure.

It is well known, today the maximum water depth at the site of the construction of bridge supports does not exceed 60 m (Akashi-Kaike Bridge [1]).

Possible places of application of such structures are the Laperouse Strait with depths of more than 50 m (the project for the creation of a transcontinental railway Europe – Japan[1] [2]), the Strait of Hormuz with depths up to 100 m, as a continuation of the North – South corridor (Ashgabat Agreement[2]) (Pic. 1 b), the Taiwan Strait with depths[3] of more than 100 m.

The possibilities of using underwater floating structures have been repeatedly considered worldwide: Funk Bay in Japan [3], Hainan Strait in China [4, 5], a floating tunnel through the Hogsfjord in Norway [6], a feasibility study of the structure at the crossing of the Strait of Messina [7]. Insufficient development of scientific problems prevented the implementation of these projects.

The possibility of using such a structure through the neck of the White Sea (Pic. 1 a, Pic. 2) with a length of about 43 km and depths of more than 100 m is considered in this article as an example. This line is promising for the transportation of export cargoes from Perm Krai [region] to Murmansk (potash fertilizers), as it will reduce the transportation distance by ~ 1000 km (by 30 %). It is known, the collapse of the bridge over the Kola River in 2020 led to a halt in supplies and the cessation of railway communication for four months[4] along the only line of the Oktyabrskaya railway. Therefore, the construction of a duplicate line through the neck of the White Sea is relevant. We also note the fundamental possibility of building such structures through Gibraltar Strait. with depths up to 1181 m and the Strait of Messina (Pic. 3), etc.

All the mentioned crossings have depths significantly exceeding the record depths of the unique Akashi-Kaike Bridge.

Despite the obvious advantages of SFT (submerged floating tunnel) structures, their design has not progressed beyond the feasibility study due to serious scientific problems. One of these problems is significant and irregular bending moments.

The *objective* of the proposed study is to optimise the design to solve the problem of overloads. To solve this problem, *methods* of structural mechanics and numerical experiment using the finite element method were used.

RESULTS

Optimisation of Bending Moments in the Radial Fastening Scheme from Constant Loads

The use of underwater floating tunnels at great depths is difficult due to the complexity of installing a large number of anchorages, although today drilling and well construction technologies are used at depths up to 3000 m [1]. Let us consider the use of radial anchor cables connected in a bunch (Pic. 4) to reduce the number of anchor attachments and to overcome obstacles at the bottom (significant depths or unsuitable soils) using such a design. Due to the compensation of the load from its own weight by the Archimedean force, the l_m span can significantly exceed the record 1100 m for cable-stayed bridges.

In Pic. 5 $l_6 = \frac{h}{\cos\alpha}$ is the length of the inclined cable, where α is the angle of inclination of the cable from the vertical, h is the length of the vertical cable.

In this analytical model (Pic. 5), to minimise the moment, it is possible to achieve the same vertical movement of the horizontal stiffening

[1] The road to Japan: Russia has proposed connecting Sakhalin and Hokkaido with a transport crossing. [Electronic resource]: https://russian.rt.com/russia/article/427017-most-sahalin-hokkaido. Last accessed 20.06.2023.

[2] Panfilova, V. Russia and Central Asian countries reset relations. Nezavisimaya Gazeta, 16.10.2022. [Electronic resource]: https://www.ng.ru/cis/2022–10–16/1_8566_asia.html?ysclid=lmt0ogwczd418645606. Last accessed 20.06.2023.

[3] [Electronic resource]: https://www.worldatlas.com/straits/taiwan-strait.html. Last accessed 20.06.2023.

[4] The renewed railway bridge over Kola river has been opened in Murmansk region. [Electronic resource]: https://tass.ru/ekonomika/9567107?ysclid=lfxsugptkg929973454. Last accessed 08.04.2023.

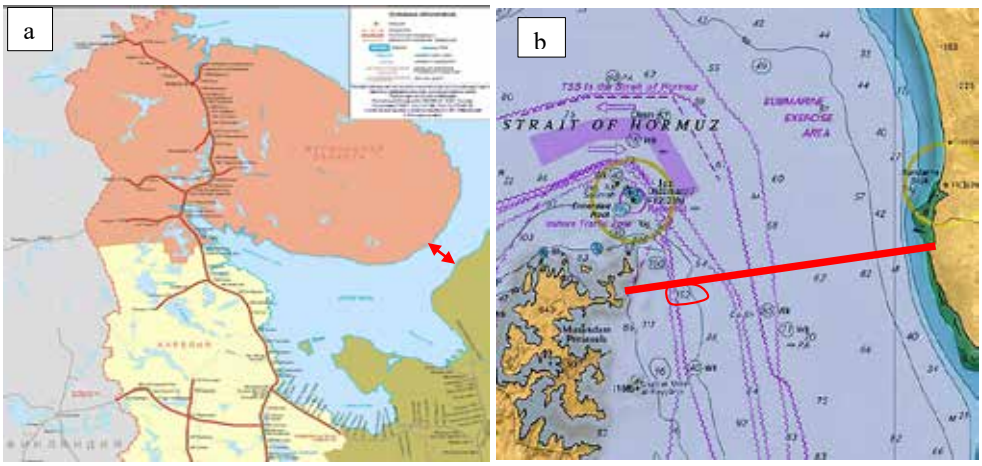

Pic. 1. The intersection of the neck of the White Sea (a) [[Electronic resource]: https://glavtrans38.com/poleznaya-informatsiya/karta-zheleznykhdorog/oktyabrskaya-zh-d/. Last accessed 20.06.2023.], the Strait of Hormuz (b) [[Electronic resource]: https://blog.geogarage.com/2019/05/strangethings-are-afoot-in-strait-of.html Last accessed 20.06.2023.], where the depths exceed 100 m.

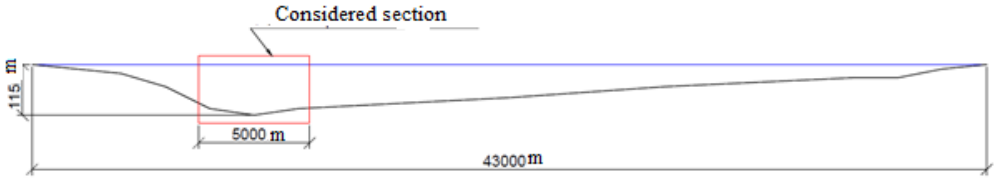

Pic. 2. The outline of the bottom of the neck of the White Sea in the station of Cape Inca [developed by the authors].

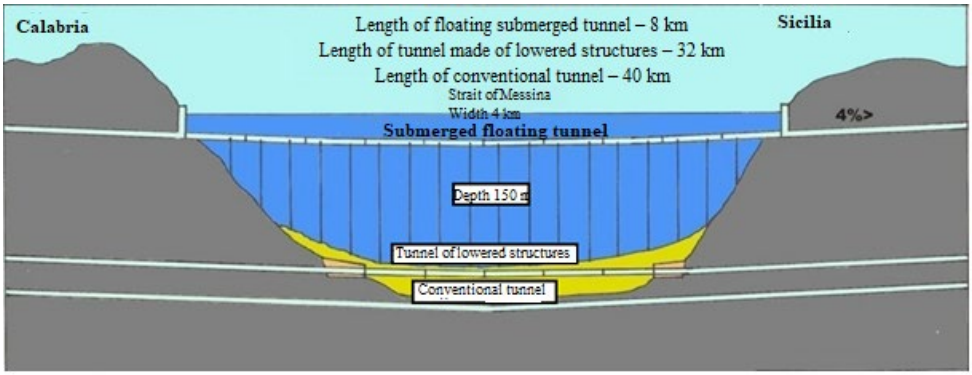

Pic. 3. Comparison of a submerged floating tunnel with other structures [1].

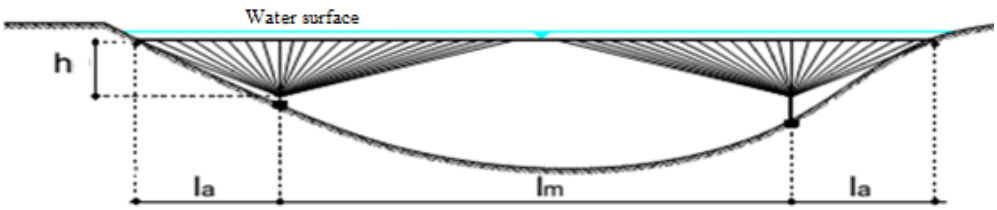

Pic. 4. Anchor cables in the radial scheme [8].

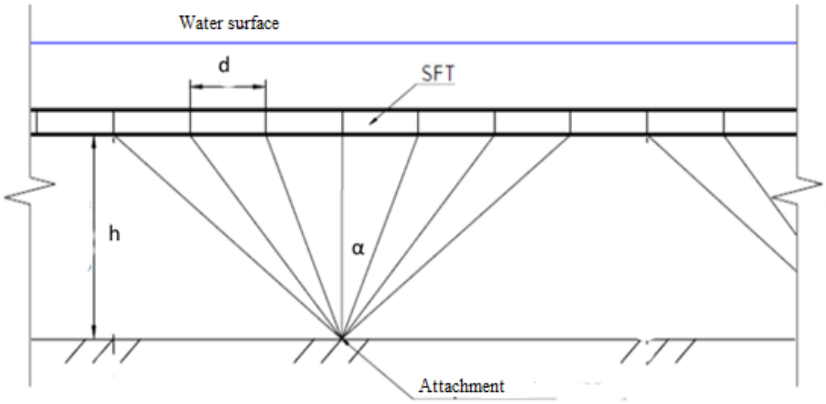

Pic. 5. The scheme of radial attachment at great depths [developed by the authors].

girder of the structure by changing the stiffness of the anchor cables depending on their angle of inclination and depth. By constant load, we will understand the sum of the loads from weight and the distributed Archimedean force. Pic. 6 shows a deformed diagram of some arbitrary node of the structure from the total constant load, while bending deformations will be considered small compared to cable deformations.

Effort in inclined tracks is

$$F_6 = \frac{F}{6os},$$

where F is the vertical component of the force in the cable.

We take $\alpha' \approx \alpha$ due to the fact that $Fn/An << E$ and $\Delta'_n << l_a$, where F_n is the force in the n-th cable, An is its cross–sectional area, E is the elastic modulus of the cable, Δ'n is the deformation of the cable, la is the length of the cable before the load is applied.

Vertical projection of the longitudinal deformation of the Δ'_n n-th inclined cable from the application of the load:

$$\Delta_n = \frac{\Delta'_n}{6os_n}.$$

To ensure equality of vertical movements of vertical and inclined cables, we assume

$\Delta_o = \Delta_1 = \Delta_2 = \ldots = \Delta_n$,

where n is the number of the cable in the girder,

$$\Delta_0 = \frac{F \cdot h}{EA}$$ – deformation of the vertical cable,

$$\Delta'_n = \frac{F_n l_n}{EA_n}$$ – deformation of the nth inclined cable,

Δ_n is the vertical projection of the inclined cable deformation,

E, A is the modulus of elasticity and the cross–sectional area of the vertical cable.

For $\Delta_o = \Delta_n$:

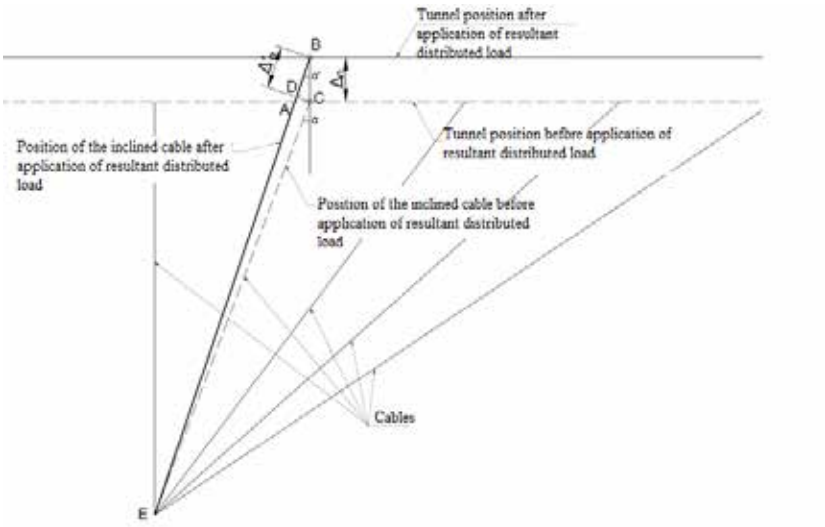

Pic. 6. A fragment of a deformed analytical model from a constant load [developed by the authors].

Table 1

Cross-sectional areas of cables for the considered model [developed by the authors]

Depth h_k, m	Angle of inclination α_{nk}, degrees	Initial cross-sectional area of cables, m^2	Cross-sectional area of cables after optimization according to the formula (3)
160	0.00	0.0683	0.0683
160	10.62	0.0683	0.0719
160	20.56	0.0683	0.0832
160	29.36	0.0683	0.1032
160	36.87	0.0683	0.1334
200	0.00	0.0683	0.0854
200	8.53	0.0683	0.0883
200	16.70	0.0683	0.0972
200	24.23	0.0683	0.1126
200	30.96	0.0683	0.1354
240	0.00	0.0683	0.1025
240	7.12	0.0683	0.1049
240	14.04	0.0683	0.1122
240	20.56	0.0683	0.1248
240	26.56	0.0683	0.1432

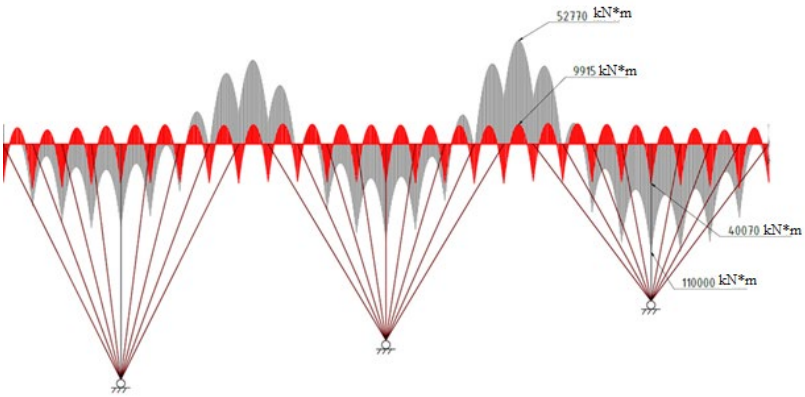

Pic. 7. Diagrams of bending moments in the structural stiffening girder from constant loads before and after optimization [developed by the authors].

$$\frac{F \cdot h}{EA} = \frac{F_n \cdot l_n}{EA \cos\varphi_n},$$

$$\frac{Fl_0}{EA} = \frac{\frac{F}{\cos\alpha}\frac{l_0}{\cos\alpha}}{EA_n \cos\alpha},$$

where A_n is the cross-sectional area of the inclined cable.

We obtain an equation providing the same vertical displacement of the structural stiffening girder for one fan attachment node:

$$EA_n = \frac{EA}{\cos^3\varphi}. \quad (1)$$

Conditions for ensuring equality of vertical displacements of the adjacent k-th bunch (Fig. 7) with a different attachment depth h_k and cross-sectional area Ak of the vertical cable:

$$\Delta_k = \Delta_0,$$

$$\frac{Fl_k}{EA_k} = \frac{Fh}{EA},$$

$$(EA)_k = \frac{EA\,h_k}{h}, \quad (2).$$

where h_k / h is the ratio of the attachment depth k of the bunch to the initial one.

Table 2

Results of optimisation of bending moments in the stiffening girder [developed by the authors]

Parameter	Before optimisation	After optimisation
Minimum moment (modulus), kNm	52770	9915
Maximum moment, kNm	110000	40070
Standard deviation, kNm	24600	8890

Substituting stiffness $(EA)_k$ of the vertical cable of the neighbouring bunch from equation (2) to equation (1) instead of the stiffness of the vertical cable *EA*, we obtain an equation that ensures the same vertical movement of the inclined cables on the *k*-th bunch:

$$(EA)_k = \frac{EA\,h_k}{h\cos^3\alpha_{nk}}, \qquad (3)$$

where α_{nk} is the angle of inclination of the nth cable in the k-th bunch. Note that the optimal solution does not depend on the parameter EJ of the stiffening girder, which can be any.

In the case of vertical cables, the optimisation task is greatly simplified.

To verify the developed method, we will perform a numerical experiment using the Katran software package based on the finite element method. To change the stiffness of the cables, we will change the cross-sectional area of the cables. The various options for the distribution of the cross-sectional area of the cables are shown in Table 1.

Table 2 shows statistical optimisation results, from which it can be seen that the minimum bending moment modulus along the length of the structure has been reduced by more than five times, the maximum bending moment has been reduced by 2.75 times, which leads to a significant reduction in material consumption. The irregularity of the moments, as can be seen from Pic. 7, is significantly reduced, which is demonstrated by a 2.8-fold decrease in the standard deviation (Table 2). This alignment of the values of bending moments will allow the use of unified sections of the structural stiffening girder.

Edge Effects on the Near-Portal Areas

The near-portal sections of the structure (near the shores of the water barrier) are located at shallow depths. In this case, the use of a radial scheme is not justified. Consider a structure with a vertical arrangement of anchor cables in the longitudinal direction. In the transverse direction, the angle of inclination of the cables to the vertical is 45^0. In this case, the rigidity of the tunnel anchors from ascent is easily determined to ensure a minimum of bending moments outside the portal sections. The plot of the moments in the stiffening girder (Pic. 8) has a significant edge effect in the coastal anchorage zone in the form of a rigid support that does not allow any movement of the stiffening girder at the place of attachment to the portal or a traditional underground tunnel.

Let's set the task of reducing bending moments in the coastal anchorage zone to a certain prescribed value. To solve this problem, we will adjust the stiffness of the cables that keep the underwater floating tunnel from surfacing in the near-portal areas.

Let's imagine a structural stiffening girder as a beam on an elastic base. The equation of the beam axis on an elastic base is

$$(EJv(x)'')'' + k(x)v(x) = q(x), \qquad (4)$$

where v(x) is a function of the deformed axis of the stiffening girder.

In this case, the first term represents the reaction of the structure to the effect of the total constant load *q(x)* due to bending of the girder, the second – due to deformation of the base (cables). From a technological point of view, it is advisable to assume *EJ = const*, the possibility of this is confirmed by the optimization results in paragraph 1 (according to expression (3), the optimal solution does not depend on EJ). In addition, for *EJ = const*, the sum of constant loads q(x) = const, since the pushing Archimedean force does not depend on x, but only on the gross cross-sectional area of the stiffening girder. Since the size of the approximation of the inner outline of the tunnel is unchanged in length, and with a decrease in the variability of the bending moment, it is possible to ensure the constancy of the area and moment of inertia of the reduced section, then

$$EJv(x)IV + k(x)v(x) = q. \qquad (5)$$

The stiffness of the base $r_t(x)$ is due to the stiffness of the cables during their longitudinal deformation:

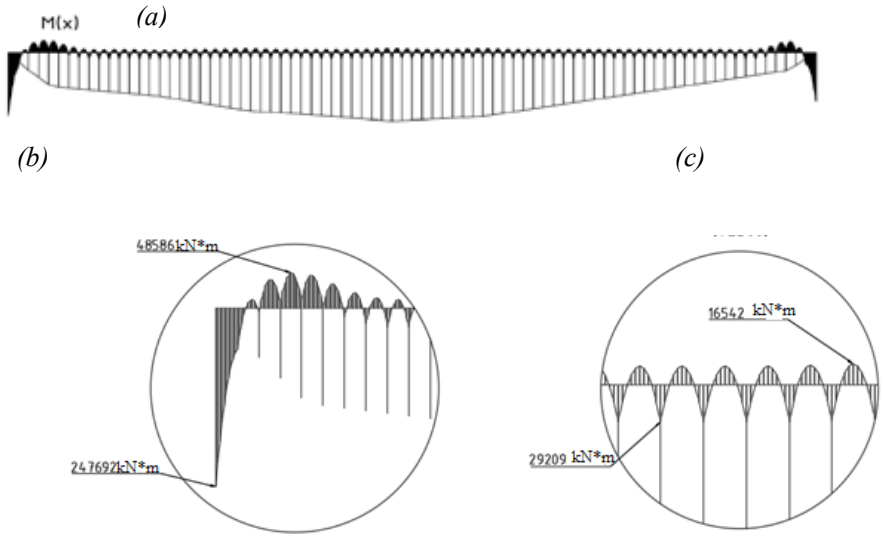

Pic. 8. Plot of moments in the structural stiffening girder (a), in the zone of the edge effect (b) and outside it (c) before optimisation [developed by the authors].

$$r_t(x) = \frac{EA(x)}{l(x)}, \quad (6)$$

where *E, A(x)* is the modulus of elasticity and the cross–sectional area of the cables,

l(x) is the length of the cables, which depends on the depth *h,*

J is the moment of inertia of the girder section relative to its horizontal axis.

Then $k(x) = r_t(x)/d$,

where *d* is the distance between the cable attachment points to the girder, and $d = const$ for technological reasons.

Pic. 8. Plot of moments in the structural stiffening girder (a), in the zone of the edge effect (b) and outside it (c) before optimisation [developed by the authors].

Based on equation (5), we obtain:

$$r_t(x) = dq / v(x) - dEJxv(x)^{IV} / v(x). \quad (7)$$

The practice of modelling the stress-strain state of a structure shows that the second term of sum of the right part (7) is 2–3 orders of magnitude smaller than the first term of sum with significant rigidity of the girder of the structure due to the need to comply with the internal clearance. In addition, to maximise the reduction of bending moments in the zone of the edge effect, and, therefore, to reduce the reaction from bending to the action of constant loads, this second term of sum should be neglected in order to avoid a significant reaction from bending, mainly shifting the perception of constant loads to anchor cables. Then, for numerical experiments to determine the stiffness function $r_t(x)$, the expression can be used:

$$r_t(x) = \frac{d \cdot q}{v(x)}. \quad (8)$$

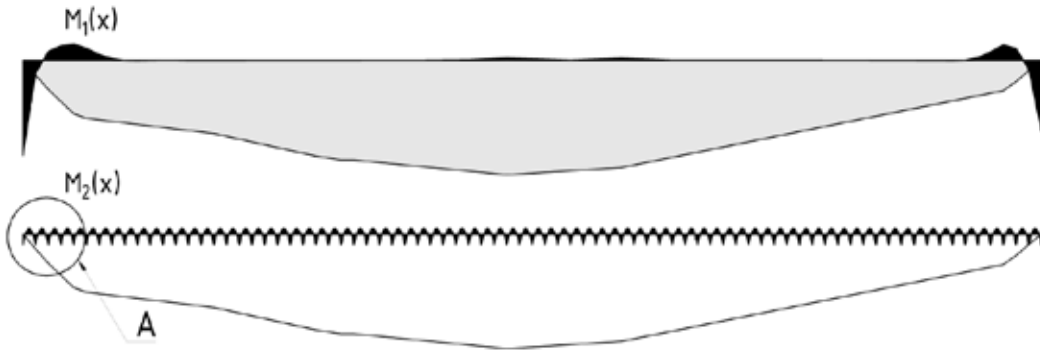

Pic. 9. Plots of moments in the presence of the edge effect (M1(x)) and in its absence (M2(x)) [developed by the authors].

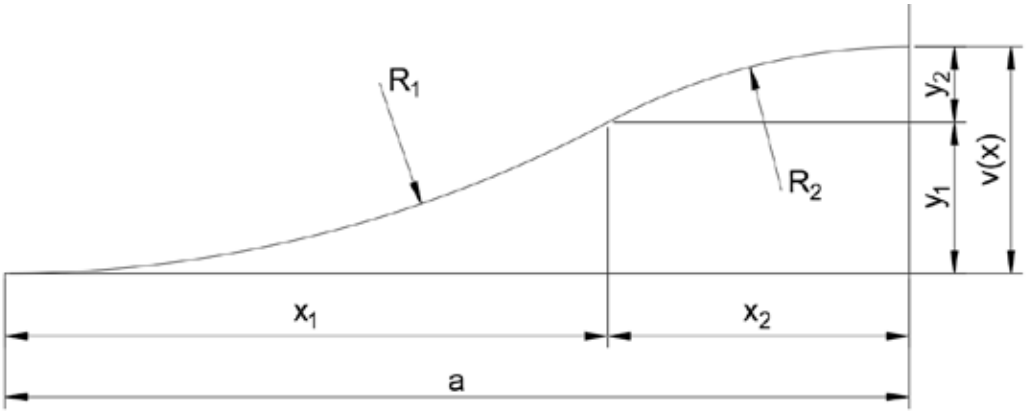

Pic. 10. Deformed axis of the stiffening girder near the shore anchorage to control the moment in the zone of the edge effect [developed by the authors].

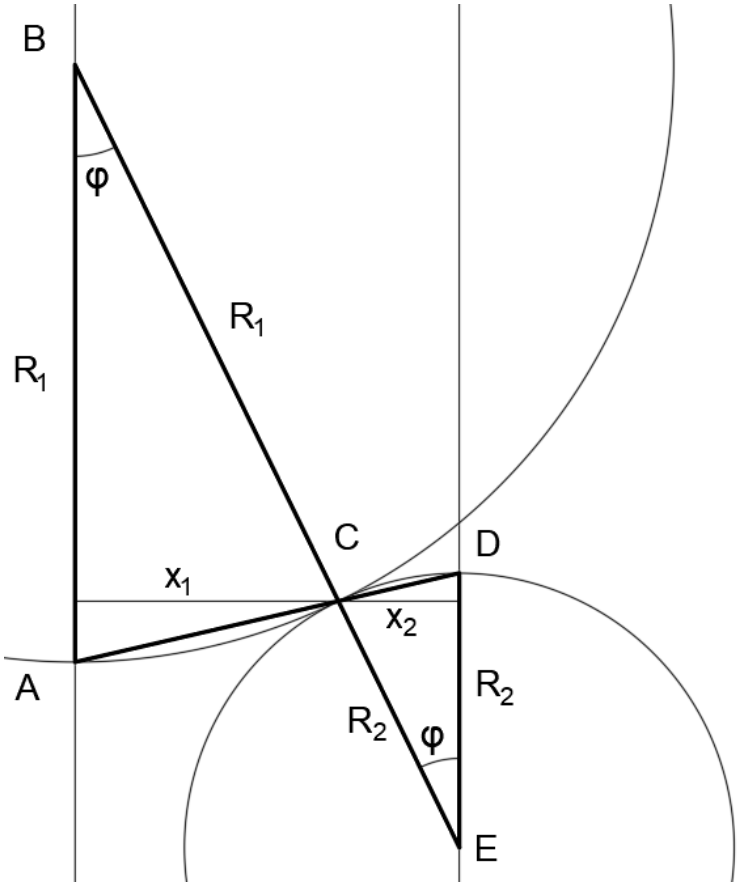

Pic. 11. The required geometry of the deformed circuit to ensure the constancy of M1 [developed by the authors].

The bending moment function M(x) can be represented as the sum (Pic. 9)

$$M(x) = M_1(x) + M_2(x), \quad (9)$$

where $M_1(x)$ describes the edge effect of shore anchoring,

$M_2(x)$ is a function of the moment, where the edge effect is insignificant.

To reduce the edge effect near the fixing points of the structural stiffening girder, we require $M_1(x)$ to be a constant bounded function (as it happens outside the edge effect zone, where M_1 is vanishing to 0). This means that the deformed axis of the girder is a circle of radius R_1 (Pic. 10) throughout x_1.

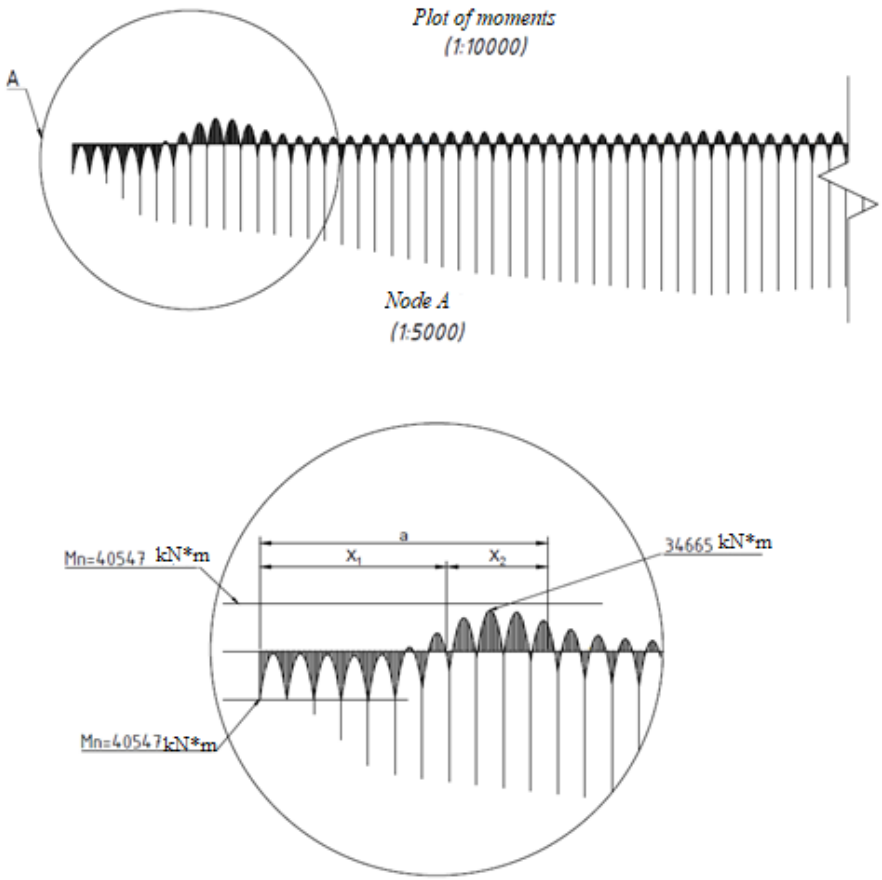

Pic. 12. Plot of moments when optimising cables of variable stiffness are used [developed by the authors].

Table 3

Parameters of a typical cable before optimisation [developed by the authors]

Name	Value
Modulus of elasticity of the cable, MPa	201000
Number of cables in the attachment unit, pcs	2
Cross-sectional area of 2 cables before optimisation, m2	0,0693
Section parameter of 2 cables, *EA*, H	1,39E+10

Then the equation of the circle over x_1 will have the form

$$R^2 = x^2 + (v(x) - R)^2. \quad (10)$$

After elementary transformations, we obtain

$$(v(x) - R)^2 = R^2 - x^2. \quad (11)$$

Or, solving the quadratic equation $v(x)^2 - 2v(x)R + x^2 = 0$, we get

$$v(x) = \pm\sqrt{R^2 - x^2} + R. \quad (12)$$

The «+» sign in (12) refers to the section of the circle with positive curvature in the right coordinate system corresponding to the section x_1, and the «–» sign refers to the section with negative curvature x_2.

Let's set $v(x)$ on the first part of the variable stiffness section such that $|M(x)|$ did not exceed a certain limiting moment M_P, i. e. $|M(x)| \le M_P$, $x \in (0; x1)$. Then, to consider this requirement, we will control the function $M_1(x)$ and take it equal $M_1(x) = M_n - \frac{qd^2}{12} = const$, where d is the distance between the cable attachment points on the section x_1 (Fig. 8). In this case, $v(x)$ is the arc of a circle $v(x) = -\sqrt{R_1^2 - x^2} + R_1$, $0 < x < x_1$.

Let's set $v(x)$ on the second part of the variable stiffness section in the same way as the first one, but with negative curvature. To consider the requirement $|M(x)| \le M_P$, $x_1 < x < x_2$, we assume $|M_1(x)| = M_n - \frac{qd^2}{12}$.

a is the length of the variable stiffness section $a = x_1 + x_2$, where x_1 and x_2 are the lengths of the first and the second parts of the variable stiffness section.

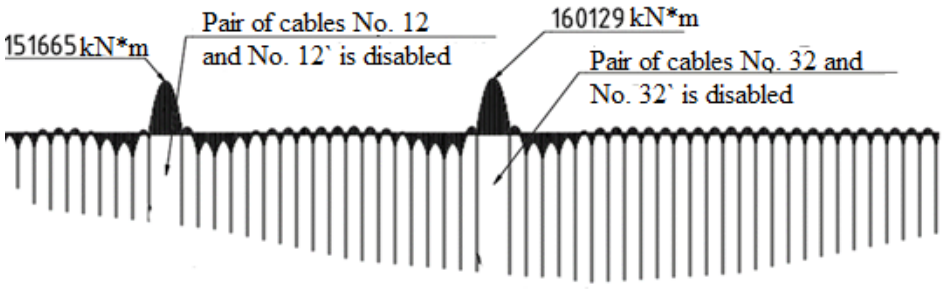

Pic. 13. Redistribution of efforts in an emergency situation of failure of two anchor cables simultaneously in each section [developed by the authors].

It is known[5] $\frac{1}{R}=\frac{M}{EJ}$, from here we find R_1 for a given moment M_1:

$$R_1=\frac{EJ}{M_{1x1}}, \quad (13)$$

where $R_1=\frac{EJ}{M_{1x1}}$ is the radius of the curve in the first section. (14)

Accordingly, $R_2=\frac{EJ}{M_{1x2}}$ the radius of the curve in the second section. (15)

From here

$$\frac{R_2}{R_1}=\frac{M_{1x1}}{M_{1x2}}=P. \quad (16)$$

Let's show that $R_1/R_2 = x_1/x_2$.

Let's construct (Pic. 11) two vertical segments AB and DE, which are parallel. BC and CE lie on the same straight line since C is the point of contact of two circles. From the fact that AB || DE, it follows that the internal intersecting angles φ are equal, and ϕ is the central angle for the half–chord x_1 and x_2. Triangles ABC and CDE are isosceles, with sides BC/CE= BA/DE = $1/R_2$.

Therefore, triangles ABC and CDE are similar due to the proportionality of the two pairs of sides and the equality of angles between them. Now consider the triangles ABC and CDE. These triangles are also similar, since all the corresponding angles of the triangles are equal. Therefore.

$$R_1 / R_2 = x_1 / x_2 = M_{1x1} / M_{1x2} = P \quad (17)$$

In this case, the values M_{1x1} и M_{1x2} are determined for reasons of *Mp* limit values (see above).

So, the function of the deformed axis of the structure in the near–portal zone has the form:

[5] Smirnov, A. F., Alexandrov, A. V., Monakhov, N. I. Strength of materials: Textbook. Ed. by A. F. Smirnov. Moscow, Higher School publ., 1975, 480 p. [Electronic resource]: https://bigenc.ru/b/soprotivlenie-materialov-b78c1d?ysclid=lmudtw94vu826302865. Last accessed 25.05.2023.

Table 4

Optimised parameters of two cables in the node (following equation (21))

N	Vertical stiffness of cables, H/m*
1	4,884E+09
2	1,221E+09
3	5,426E+08
4	2,805E+08
5	1,903E+08
6	1,323E+08
7	9,728E+07
8	7,858E+07
9	6,946E+07
10	6,547E+07
11	6,401E+07
12	6,265E+07
13	6,135E+07

Table 5

Results of optimisation of bending moments in the structural stiffening girder [developed by the authors]

Parameter	Before optimisation	After optimisation
Minimum moment (modulus), kNm	48 586	34 665
Maximum moment, kNm	247 692	40 547

$$v(x)=-\sqrt{R_1^2-x^2}+R_1,\ x\in(0;x_1), \quad (18)$$

$$v(x)=\sqrt{R_2^2-(x-a)^2}+R_2,\ x\in(x_1;a), \quad (19)$$

where $x_1=\frac{a(x)}{1+P}$,

$$a(x)=\sqrt{R_1^2-\left(\frac{h(x)dq}{EA(1+P)}-R_1\right)^2(P+1)}, \quad (20)$$

A is the constant cross-sectional area of the cable before optimization.

Knowing the deflection function (18) and (19), we will find the required rigidity of fastening with cables to reduce the edge effect:

$$r_t(x)=\frac{EA(x)}{l(x)}=\frac{dq}{v(x)}. \quad (21)$$

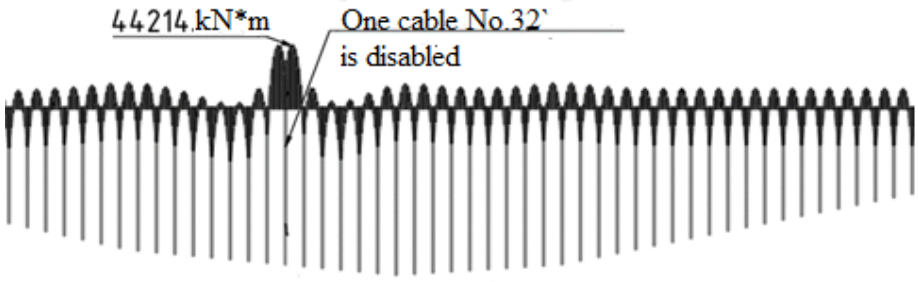

Pic. 14. Redistribution of efforts in an emergency of failure of one anchor cable [developed by the authors].

Table 6

Changes in longitudinal forces in cables in two emergency situations [developed by the authors]

Cable number	№ 31	№ 32	№ 33
Force to breakage, kN	7313	7314	7318
The force after breaking two cables, kN	9499	-	9477
The force after breaking one cable, kN	7890	10765	7888

Verification of the Optimisation Method

To verify the method of optimising the structure to minimise the bending moment in the stiffening girder of the structure, a numerical experiment was performed using the Katran software package based on the finite element method. In the considered scheme, the cables are arranged in pairs along the tunnel in increments of 30 m, the depth of the water barrier is up to 300 m, and the width is 2.5 km. The cross-sectional area can always be provided with a set of parallel cables. The parameters of the cable located vertically in the longitudinal projection before optimization are indicated in the Table 3. Limit the value of the maximum modulo moment to 40547 kNm.

We will find the necessary stiffness of the cables in a section of variable stiffness according to the formula (21). The optimised parameters of the cables are shown in Table 4. Pic. 11 shows a plot of moments in the stiffening girder of the structure. As can be seen from the comparison of plots before optimization (Pic. 8) and after optimization (Fig. 12), the edge effect of shore fastening of the stiffening girder is significantly reduced.

Obviously, in the case of a significant required cross-sectional area, cable packages or other structures will be used.

Table 5 shows the comparative parameters of the stress-strain state (bending moments) before and after optimisation according to the proposed method. As can be seen from Table 5, the maximum bending moment has been reduced by more than 6 times, the minimum moment by more than 1,4 times. It can be seen from the table that the maximum value of the bending moment does not exceed the specified limit of 40547 kNm.

Survivability of the Structure

Survivability is the property of an object to remain operational in the presence of defects or damage of a certain type, as well as in case of failure of some components[6]. Let's consider two cases of failure of individual anchoring cables of the structural stiffening girder due to the destruction of the anchorage, the breakage of two cables or one cable. The first calculation case seems unlikely due to the location of anchors on the bottom at a distance of at least nine meters (diameter of a single girder of a single-track structure) with vertical anchor cables. In fact, in the transverse projection, the cables have an incline to ensure the transverse stability of the girder under the action of temporary loads (vibration of rolling stock, currents, the effect of surface waves). This leads to an even greater distance between the anchors, and, therefore, to a decrease in the probability of destruction of two anchor fastenings of the girder at the same time. The failure of two cables at the same time is unlikely but deserves consideration.

In the first case, there is a redistribution of bending moments, shown in Pic. 13. As can be seen from the comparison of Pic. 8 and Pic. 13, bending moments increase almost tenfold. Note, however, that the increase in bending moment is approximately the same at different attachment points and does not depend on the depth (length of the cables). Thus, the unification of the

[6] GOST [State Standard] R 27.102–2021. Dependability in technics. Dependability of item. Terms and definitions. [Electronic resource]: https://hseblog.ru/kb/document/3094/files/12625/ГОСТ%20Р%2027.102–2021 %20Надежность%20в%20технике.%20Надежность%20объекта.%20termines %20and %20determinations_Text.pdf?ysclid=lmug1h8vsb527543341. Last accessed 25.05.2023.

assembly sections of the stiffening girder, achieved in paragraph 1, remains, even if strength is calculated in this emergency. The overloads associated with the failure of the anchor cables remain local (Pic. 13). Note also that due to the opposite direction of the constant loads and the temporary load from the rolling stock, the presence of rolling stock will reduce overloads. Thus, even in the case of an emergency in question, the movement cannot be completely stopped. It is important to ensure the strength of the girder in this emergency due to its significant height exceeding nine meters to comply with the internal clearance.

The second calculation case, associated with the failure of one of the anchor cables, seems more likely. In this case (Pic. 14), the bending moments increase to a much lesser extent than in the first calculated case. The negative moment increases approximately 2.6 times in comparison with the standard situation (Pic. 8).

The change in longitudinal forces in anchor cables in emergency situations is shown in Table 6. In case of simultaneous breakage of two cables, the forces in adjacent cables increase by 30 %, in case of failure of one cable, the force in the remaining cable from the pair increases by 47 %. In this case, when rolling stock appears, cable overloads will decrease, i. e., an emergency will allow trains to continue moving.

Considering the indicated redistribution of internal forces, the survivability of the structure will be ensured.

CONCLUSIONS

The article substantiates the operability of a submerged floating transport structure. An engineering method has been developed to optimise bending moments in the stiffening girder of an submerged floating transport structure, which allows several times to reduce bending moments in the zones of the near-port sections, as well as significantly reduce bending moments in deep-water sections with radial anchoring of anchor cables. This solution makes it possible to use unified sections of the structural stiffening girder during construction.

The survivability of the structure can be ensured both in case of failure of one or two anchor cables, while the load from the train reduces overloads from constant loads due to the opposite direction of the resultant constant loads and the temporary load from the rolling stock, i. e., the presence of rolling stock will reduce overloads. Thus, even in the case of an emergency in question, the traffic will not be completely stopped.

REFERENCES

1. Poliakov, V. Yu., Khorev, I. V., Demidov, I. M. Modern approaches to the study and development of underwater floating structures. Transport structures [Transportnye sooruzheniya], 2022, Vol. 9, Iss. 3, Art. 7. DOI: 10.15862/08SATS322.

2. Vinokurov, M. A., Sukhodolov, A. P. Economics of Irkutsk region. £ vols. Irkutsk, BGUEP (IGEA) publ., 2002, Vol. 3, 432 p. ISBN 5-7253-0677-1. [Electronic resource]: https://opac.nsuem.ru/mm/2015/000212732.pdf. Last accessed 27.05.2023.

3. Maeda, N., Morikawa, M., Ishikawa, K., Kakuta, Y. Study on structural characteristics of support systems for submerged floating tunnel. Proceedings of the 3rd Symposium on Strait Crossings, Ålesund, Norway, 1994, pp. 579–674. [Electronic resource]: https://www.gbv.de/dms/tib-ub-hannover/193950901.pdf. Last accessed 25.04.2023.

4. Martinelli, L., Barbella, G., Feriani, A. Modeling of Qiandao Lake submerged floating tunnel subject to multi-support seismic input. *Procedia Engineering*, 2010, Vol. 4, pp. 311–318. DOI: 10.1016/j.proeng.2010.08.035.

5. Mazzolani, F., Landolfo, R., Faggiano, B., Esposto, M., Martire, G., Perotti, G. Structural Analyses of the Submerged Floating Tunnel Prototype in Qiandao Lake (PR of China). *International Journal Advances in Structural Engineering*, 2008, Vol. 11, Iss. 4, pp. 439–454. DOI: 10.1260/136943308785836862.

6. Skopra, L. Innovative Norwegian fjord crossing. How to cross the Høgsjord, alternative methods. Proceedings of the 2nd Congress AIOM (Marine and Offshore Engineering Association), Naples, Italy, 1989. [Electronic resource]: https://www.matec-conferences.org/articles/matecconf/ref/2017/52/matecconf_eacef2017_02026/matecconf_eacef2017_02026.html. Last accessed 25.04.2023.

7. Bruschi, R., Giardinieri, V., Marazza, R., Merletti, T. Submerged Buoyant anchored Tunnels: Technical Solution for the Fixed Link across the Strait of Messina Italy. Proceedings of the 2nd Symposium on Strait Crossings. Balkema, Rotterdam, Netherland. 1990. pp. 605–612.

8. Jin, Chungkuk, Kim Hansung. Dynamic Responses of a Submerged Floating Tunnel in Survival Wave and Seismic Excitations. Proceedings of the 27th International Ocean and Polar Engineering Conference, San Francisco, CA, USA, 25–30 June 2017. International Society of Offshore and Polar Engineers, 2017, pp. 547–551. DOI: 10.12989/OSE.2017.7.1.001.

Information about the authors:

Demidov, Ivan M., *Ph.D. student at the Department of Bridges and Tunnels of Russian University of Transport, Moscow, Russia, dmdvn@rambler.ru.*

Poliakov, Vladimir Yu., *D.Sc. (Eng), Professor at the Department of Bridges and Tunnels of Russian University of Transport, Moscow, Russia, pvy55@mail.ru.*

Article received 13.06.2023, approved 15.11.2023, accepted 17.11.2023.